doi:10.1016/j.jmb.2008.09.070 J. Mol. Biol. (2008) 384, 896–907

JMB

Available online at www.sciencedirect.com

ScienceDirect

ELSEVIER

Ubiquitin-Proteasome System Impairment Caused by a Missense Cardiac Myosin-binding Protein C Mutation and Associated with Cardiac Dysfunction in Hypertrophic Cardiomyopathy

Udin Bahrudin[1,2], Hiroko Morisaki[3], Takayuki Morisaki[3], Haruaki Ninomiya[4], Katsumi Higaki[5], Eiji Nanba[5], Osamu Igawa[6], Seiji Takashima[7], Einosuke Mizuta[6], Junichiro Miake[1], Yasutaka Yamamoto[1], Yasuaki Shirayoshi[1], Masafumi Kitakaze[8], Lucie Carrier[9,10] and Ichiro Hisatome[1]*

[1]*Division of Regenerative Medicine and Therapeutics, Institute of Regenerative Medicine and Biofunction, Tottori University Graduate School of Medical Science, Yonago, Japan*

[2]*Department of Cardiology and Vascular Medicine, Medical Faculty Diponegoro University and Dr. Kariadi Hospital, Semarang, Indonesia*

[3]*Department of Bioscience, National Cardiovascular Center Research Institute, Osaka, Japan*

[4]*Department of Biological Regulation, Tottori University Faculty of Medicine, Yonago, Japan*

[5]*Division of Functional Genomics, Research Center for Bioscience and Technology, Tottori University, Yonago, Japan*

[6]*Division of Cardiology, Tottori University Hospital, Yonago, Japan*

The ubiquitin-proteasome system is responsible for the disappearance of truncated cardiac myosin-binding protein C, and the suppression of its activity contributes to cardiac dysfunction. This study investigated whether missense cardiac myosin-binding protein C gene (*MYBPC3*) mutation in hypertrophic cardiomyopathy (HCM) leads to destabilization of its protein, causes UPS impairment, and is associated with cardiac dysfunction. Mutations were identified in Japanese HCM patients using denaturing HPLC and sequencing. Heterologous expression was investigated in COS-7 cells as well as neonatal rat cardiac myocytes to examine protein stability and proteasome activity. The cardiac function was measured using echocardiography. Five novel *MYBPC3* mutations—E344K, ΔK814, Δ2864-2865GC, Q998E, and T1046M—were identified in this study. Compared with the wild type and other mutations, the E334K protein level was significantly lower, it was degraded faster, it had a higher level of polyubiquination, and increased in cells pretreated with the proteasome inhibitor MG132 (50 μM, 6 h). The electrical charge of its amino acid at position 334 influenced its stability, but E334K did not affect its phosphorylation. The E334K protein reduced cellular 20 S proteasome activity, increased the proapoptotic/antiapoptotic protein ratio, and enhanced apoptosis in transfected Cos-7 cells and neonatal rat cardiac myocytes. Patients carrying the E334K mutation presented significant left ventricular dysfunction and dilation. The conclusion is the missense *MYBPC3* mutation E334K destabilizes its protein through UPS and may contribute to cardiac dysfunction in HCM through impairment of the ubiquitin-proteasome system.

*Corresponding author. E-mail address: hisatome@med.tottori-u.ac.jp.

Abbreviations used: HCM, hypertrophic cardiomyopathy; *MYBPC3*, cardiac myosin-binding protein C gene; cMyBP-C, cardiac myosin-binding protein C protein; Wt, wild type; UPS, ubiquitin-proteasome system; NRCM, neonatal rat cardiac myocyte; RT-PCR, real-time polymerase chain reaction; FACS, flow cytometry.

0022-2836/$ - see front matter © 2008 Elsevier Ltd. All rights reserved.

[7]*Department of Molecular Cardiology, Osaka University Graduate Scholl of Medicine, Suita, Osaka, Japan*

[8]*Department of Cardiovascular Medicine, National Cardiovascular Center, Suita, Osaka, Japan*

[9]*Institute of Experimental and Clinical Pharmacology and Toxicology, University Medical Center Hamburg-Eppendorf, Hamburg, Germany*

[10]*UPMC Univ Paris 06, UMR_S582, IFR14, Paris, F-75013, France*

Received 5 May 2008; received in revised form 9 September 2008; accepted 22 September 2008
Available online
7 October 2008

Edited by M. Yaniv

Keywords: hypertrophic cardiomyopathy; cardiac myosin-binding protein C; missense mutation; ubiquitin-proteasome system; cardiac dysfunction

Introduction

Hypertrophic cardiomyopathy (HCM) is inherited as a Mendelian autosomal dominant trait and is caused by mutations in any of the 13 genes encoding proteins of the cardiac sarcomere and the non-cardiac sarcomeric protein.[1,2] In several studies, mutations in the cardiac myosin-binding protein C gene (*MYBPC3*) were found to be one of the two commonest genetic causes of familial HCM.[3–6] To date, more than 150 mutations have been identified in *MYBPC3*, consisting of missense, deletion/insertion, and splice site abnormalities. cMyBP-C, a 144 kDa protein, has a modular structure consisting of 11 globular domains composed of eight immunoglobulin I motifs, three fibronectin type III repeats, and the MyBP-C motif containing three phosphorylation sites;[7] it is a major component of thick filaments in the C-zone of the A-band of the sarcomere; it stabilizes the sarcomere structure and modulates cardiac contractility controlled by phosphorylation, which in turn depends on adrenergic stimulation and cAMP-regulated protein kinase.[7,8]

Mutations in *MYBPC3* are often associated with a translational frameshift leading to truncated proteins.[4,9,10] In a number of independent studies, the expected proteins were not seen in Western blots of the cardiac tissue of patients known to be carriers of frameshift *MYBPC3* mutations, suggesting the truncated protein is removed rapidly from the cell by proteolytic degradation in addition to the poisonous polypeptide mode of action or haploinsufficiency.[11–14] Sarikas *et al.* reported recently that the ubiquitin-proteasome system (UPS) was responsible for the disappearance of truncated cMyBP-C.[15] Moreover, they observed that UPS impairment was a consequence of its encounter with truncated cMyBP-C. Inhibition of UPS has been hypothesized to have an important role in the progression of cardiovascular disease, since Tsukamoto *et al.* demonstrated that suppression of proteasome activity contributed to cardiac dysfunction due to apoptosis of cardiomyocytes resulting from accumulation of proapoptotic proteins by impaired degradation.[16] However, there are no reports that the missense *MYBPC3* mutation discovered in human hypertrophic cardiomyopathy causes instability of cMyBP-C, leading to UPS impairment. In this study, we found the missense *MYBPC3* mutation identified in three patients with HCM caused instability of its protein, which is degraded by UPS. Interestingly, expression of this mutant protein led to UPS impairment characterized by reduction of 20 S proteasome activity, increased the proapoptotic/antiapoptotic protein ratio, and enhanced apoptosis. We found that HCM patients with this mutation presented cardiac dysfunction.

Results

Novel mutations and polymorphisms in *MYBPC3*

Screening of the exons and flanking sequences of human *MYBPC3* led to five novel mutations, three

Table 1. Identified mutations and polymorphisms of *MYBPC3* gene in Japanese patients with hypertrophic cardiomyopathy

Mutation / SNP No.	Base	Amino acid	Exon/intron	Allele	Note
1	G1022A	Glu334Lys (E334K)	Ex. 12	ht	Novel mutation
2	2472-2474AAGdel	Lys814del (ΔK814)	Ex. 25	ht	Novel mutation
3	2864-2865GCdel, frame shift+ stop codon	Loss of the terminal 207 amino acid residues (16.2%)	Ex. 27	ht	Novel mutation
4	C3024G	Gln998Glu (Q998E)	Ex. 28	ht	Novel mutation
5	C3169T	Thr1046Met (T1046M)	Ex. 29	ht	Novel mutation
6	C65T	Ala11Ala (A11A)	Ex. 2	hm	Reported SNP[a]
7	G121A	Glu30Glu (E30E)	Ex. 2	ht	Novel SNP
8	G146A	Val38Val (V38 V)	Ex.2	ht	Novel SNP
9	G232C	Arg67Thr (R67T)	Ex.2	ht	Novel SNP
10	del/ins C	–	In. 4	ht	Reported SNP[a]
11	A738G	Ser236Gly (S238G)	Ex. 6	ht	Reported SNP[a]
12	C2579T	Val849Val (V849V)	Ex. 25	ht	Reported SNP[a]
13	G2491A	Arg820Gln (R820Q)	Ex. 25	ht	Reported SNP[a]
14	G3320A	Glu1096Glu (E1096E)	Ex. 30	hm/ht	Reported SNP[a]

hm, homozygous; ht, heterozygous; SNP, single nucleotide polymorphism.
[a] Reported at http://www.ncbi.nlm.nih.gov/SNP/snp_ref.cgi?locusId=4607&chooseRs=all.

novel and six reported polymorphisms in 30 Japanese patients with HCM (Table 1). These mutations were not observed in 100 unrelated healthy Japanese individuals. Among them, a Glu334Lys (E334K) missense mutation (Fig. 1) was identified in three patients from different families. This mutation was located in the MyBP-C motif, in the region between C1 and C2, which has a phosphorylation-dependent regulatory function.[17] The other missense mutations, Q998E and T1046M, were located in the C8 region that has a binding site for titin.[18] ΔK814 caused the loss of an amino acid in the C6 region. Δ2864-2865GC caused the loss of the terminal 332 amino acid residues, including the myosin/titin-binding region, and was replaced by 125 novel residues, which is truncation by about 16.2% of the length of the wild type (Wt). Segregation of the mutation was not possible, since we had no access to the relatives. No mutation of other candidate genes involving myosin heavy chain was found in the patients carrying *MYBPC3* mutations.

Decreased level of the E334K mutant cMyBP-C protein through UPS

Wt myc-cMyBP-C expressed in COS-7 cell as well as neonatal rat cardiac myocyte (NRCM) was detected by anti-myc Western blotting at 144 kDa, the predicted size of full-length myc-cMyBP-C. Although comparable with the abundance of Wt cMyBP-C mRNA (Fig. 2b; Supplementary Data Fig. 1c), the level of the E334K mutant protein was 44±6% less ($p<0.05$) compared with Wt (Fig. 2a; Supplementary Data Fig. 1a). The protein levels of other cMyBP-Cs mutants including ΔK814, Δ2864-2865GC, Q998E, and T1046M, were comparable with the level of Wt (Fig. 2a; Supplementary Data Fig. 1b). myc-cMyBP-C was recovered in the detergent-soluble fraction, excluding any mutation-induced change in protein solubility (data not shown). Treatment with MG132 (50 μM for 6 h) increased the density of the band of the E334K mutant protein significantly, to a density comparable with that of Wt myc-cMyBP-C protein (Fig. 2c). MG132 increased the

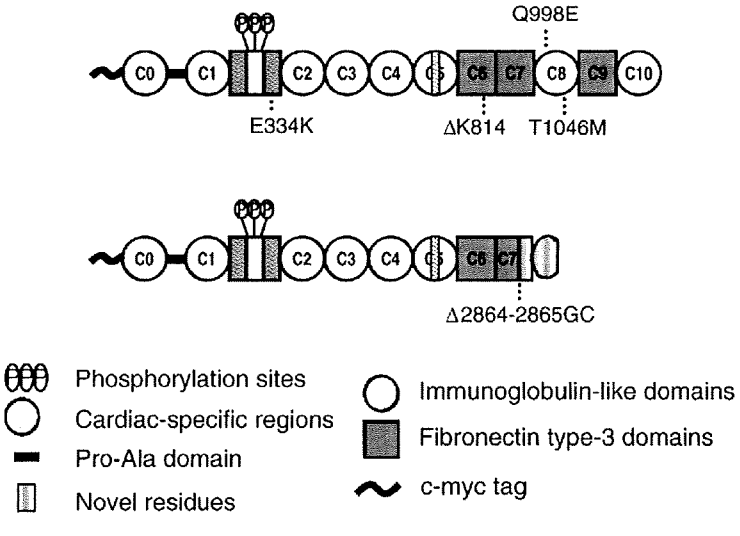

Fig. 1. Diagram of the general organization of mutant cMyBP-Cs. The full-length Wt cMyBP-C contains 1273 amino acids, and is composed of eight immunoglobulin-I motifs, three fibronectin type III repeats, and the MyBP-C motif containing three phosphorylation sites. The E334K, ΔK814, Q998E, T1046M, and Δ2864-2865GC positions are indicated. Δ2864-2865GC caused a loss of the terminal 332 amino acid residues and their replacement by 125 novel residues (truncation by about 16.2% of Wt length).

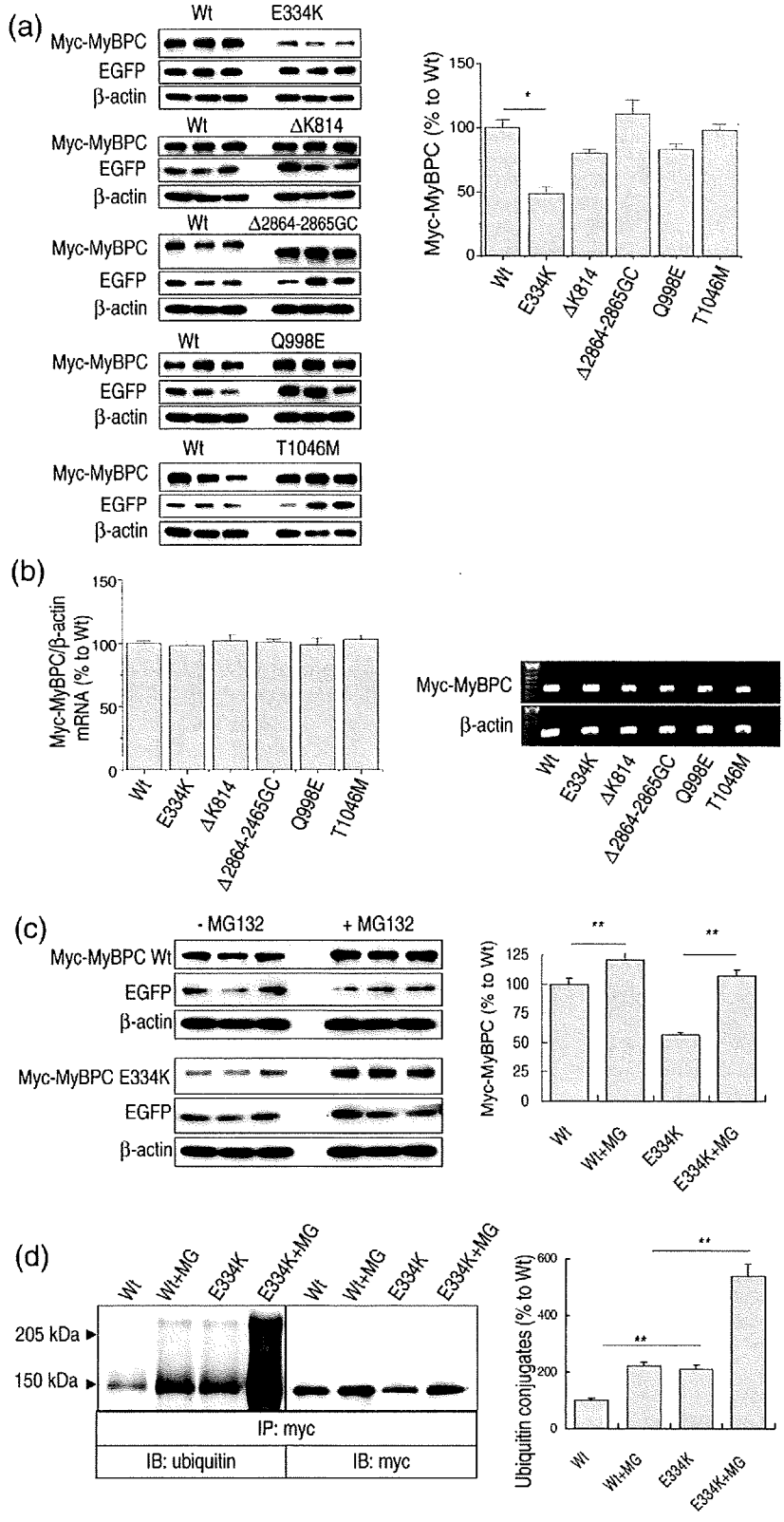

Fig. 2. Decreased level of the E334K mutant cMyBP-C protein through UPS. (a) Western blot analysis with the indicated antibodies found to be over-expressed cMyBP-Cs. Protein extracts of COS-7 cells were prepared 48 h after co-transfection with the indicated mutant *MYBPC3* and EGFP plasmid. Left, representative Western blot; right, quantitative densitrometric scan of myc-MyBP-Cs compared to the Wt, $n=10$. (b) Left, quantitative real-time PCR of human cMyBP-C mRNA expressed in COS-7 cells transfected with either Wt or mutant *MYBPC3* plasmid constructs, $n=5$. Right, PCR amplification product of the cDNAs, β-actin mRNA level served as control. (c) Increased level of E334K mutant protein by pretreatment with the proteasome inhibitor MG132. Western blot analysis of Wt and mutant cMyBP-Cs with the indicated antibody after co-transfection with either Wt or E334K and EGFP constructs, in the absence or after treatment with the proteasome inhibitor MG132 (50 μM, 6 h). Left, the representative Western blot; right, quantitative densitrometric scan of myc-MyBP-Cs compared to the Wt, $n=6$. (d) Cell lysates from COS-7 transfected with either Wt or E334K, in the absence or after treatment with the proteasome inhibitor MG132 (50 μM, 6 h). Anti-myc immunoprecipates (IP) were subjected to immunoblotting (IB) with anti-ubiquitin or anti-myc. Left, the representative blots, molecular mass is indicated on the left-hand side (kDa); right, quantitative densitrometric scan of ubiquinated myc-MyBP-Cs compared to the Wt, $n=6$. (a and c) EGFP was quantified for controlling minor inter-individual differences in transfection efficiency, and β-actin was determined as control of protein loading. $^{*}p<0.05$, $^{**}p<0.001$.

protein level of Wt myc-cMyBP-C significantly as well, while its extent was smaller than of the E334K protein. myc-cMyBP-C was recovered in the detergent-soluble fraction in the absence and in the presence of MG132, excluding MG132-dependent changes of protein solubility (data not shown). Immunoprecipitation

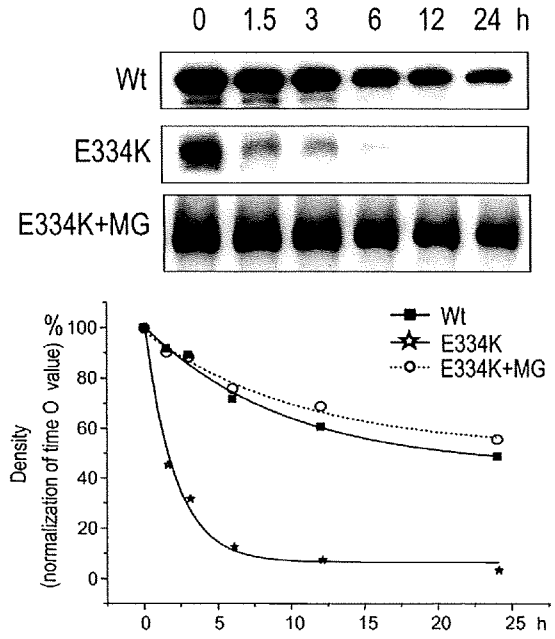

Fig. 3. Fast degradation process of E334K mutant cMyBP-C protein. Wt and E334K cMyBP-C transfected COS-7 cells were pulse-labeled with [^{35}S]methionine and chased for the indicated times. Anti-myc immunoprecipitates (IP) were subjected to autoradiography. Representative autoradiographs (top) and plots of the decay curve (bottom) illustrating the protein degradation process and its time-course relative to Wt are shown. The half-life of the Wt, E334K, and E334K treated with MG132 (0.5 μM) were 9.55±2.059 h, 2.01±0.26 h, and 10.46±2.68 h, respectively. The blots were normalized to 100% at time zero. Six replicates gave similar results.

experiments showed that the level of polyubiquitination of the E334K mutant of myc-cMyBP-C protein was significantly higher than that of Wt (Fig. 2d). MG132 treatment (50 μM for 6 h) increased the level of ubiquitinated E334K mutant myc-cMyBP-C significantly, and its extent was greater than that of Wt.

Fast degradation process of E334K mutant cMyBP-C protein

To investigate the stability of the E334K mutant myc-cMyBP-C protein, we determined a half-life of expressed protein by pulse–chase analysis. Figure 3 shows the degradation process of both Wt and E334K mutant proteins. The E334K mutant protein was degraded significantly faster with a half-life ($t_{1/2}$) of 2.01±0.26 h, compared to the Wt $t_{1/2}$ of 9.55±2.059 h. Pretreatment with MG132 (0.5 μM) prolonged the $t_{1/2}$ of the E334K mutant protein to 10.46±2.68 h. On the other hand, the four mutant myc-cMyBP-Cs ΔK814, Δ2864-2865GC, Q998E, and T1046M had the same $t_{1/2}$ as the Wt (data not shown). The proteasome inhibitor lactacystine (25 μM) and proteasome inhibitor 1 (100 μM) had similar effects, whereas the lysosomal inhibitor chloroquine (2 mM), had no effect (data not shown).

Electrical charge of the amino acid at position 334 of cMyBP-C influenced protein stability

The type and position of the mutation in the gene influences protein structure and stability.[19] Since glutamic acid (E) was negatively charged and lysine (K) was positively charged, the E334K mutant caused an amino acid charge change of+2 in myc-cMyBP-C, which may have affected its stability. The effect of substituting the electrical charge of the amino acid at position 334 with different electrical charges, i.e. aspartic acid (D, negative charge), glutamine (Q, uncharged), and glycine (G, non-polar) on the expression level of the protein was investigated. Replacement of E by D (negative to negative) restored the protein expression significantly, to a level similar to the Wt, although replacement of E by Q or G (negative to uncharged or non-polar) partially restored the expression level of the protein (Fig. 4a), despite a comparable level of mRNA (Fig. 4b), indicating that the negatively charged amino acid E could be responsible for the stability of myc-cMyBP-C. Although this region includes its phosphorylation site, there was no difference in phosphorylation between the E334K mutant and Wt myc-cMyBP-Cs (Fig. 4c).

Expression of E334K mutant cMyBP-C protein is associated with impaired UPS

It is well known that ubiquitinated protein accumulates in cells when UPS is deactivated. As the ubiquitinated form of E334K mutant protein was increased significantly (Fig. 2d), the expression of E334K mutant cMyBP-C was thought to be associated with UPS impairment characterized by decreased 20 S proteasome activity, increased level of pro-apoptotic-regulating proteins, and increased apoptosis. To investigate the effect of E334K mutant cMyBP-C on UPS, we performed transient transfection into NRCM and generated stable Wt and mutant myc-cMyBP-C transfectants of Cos-7 cells. As shown in Fig. 5a and Supplementary Data Fig. 2a, 20 S proteasome activity, i.e. chymotrypsin-like activity, was significantly lower in the stable E334K mutant myc-cMyBP-C transfectants of cells in comparison with that in the Wt cells. On the other hand, there was no difference in these parameters between Wt and other mutants. Figure 5b and Supplementary Data Fig. 2b show the results of Western blot analysis with anti-p53, anti-Bax, anti-cytochrome *c*, anti-Bcl-2 and anti-Bcl-xL detected the corresponding proteins in either Wt or the E334K mutant myc-cMyBP-C stable transfectants of Cos-7 cells and NRCM, respectively. The E334K mutant myc-cMyBP-C increased expression of pro-apoptotic-regulating proteins significantly (p53, Bax, and cytochrome *c*) and reduced expression of anti-apoptotic-regulating proteins (Bcl-2 and Bcl-xL) in comparison with Wt associated with decreased level of E334K mutant myc-cMyBP-C. The population of Sub-G1 phase corresponding to apoptosis was significantly higher in the stable E334K mutant myc-cMyBP-C transfectants of

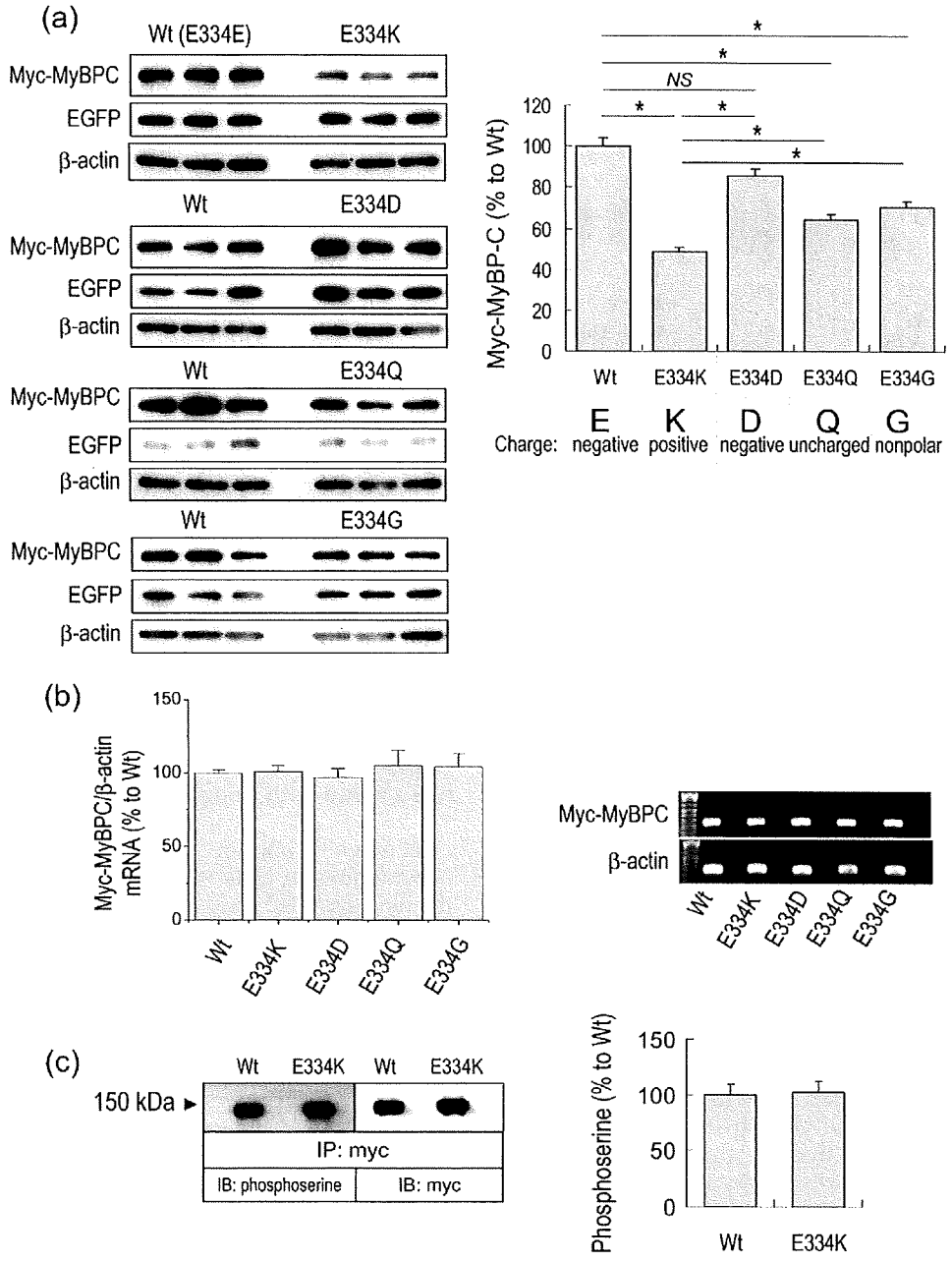

Fig. 4. Electrical charge of the amino acid at position 334 influenced the protein stability. In addition to Wt and E334K, three plasmid constructs encoding myc-cMyBP-Cs with different electrical charges of the amino acid at position 334 were generated (E334D, E334Q, and E334G). (a) Protein extracts from COS-7 cells were prepared 48 h after co-transfection with Wt, E334K, E334D, E334Q, E334G, and EGFP constructs. Left, representative Western blot, EGFP was quantified for controlling minor inter-individual differences in transfection efficiency, and β-actin was the control for protein loading; right, quantitative densitrometric scan of myc-MyBP-Cs compared to the Wt, $n=6$. (b) Left, quantitative real-time PCR of human cMyBP-C mRNA expressed in COS-7 cells transfected with either Wt or mutant *MYBPC3* plasmid constructs, $n=5$. Right, PCR amplification product of the cDNAs, β-actin mRNA served as control. (c) Cell lysates from COS-7 transfected with Wt and E334K. Anti-myc immunoprecipates (IP) were subjected to immunoblotting (IB) with anti-phosphoserine or anti-myc antibody. Left, the representative blots, molecular mass is indicated on the left (kDa); right, quantitative densitrometric scan of phosphorylated E334K mutant cMyBP-C protein compared to the Wt, $n=6$. Molecular mass is indicated on the left-hand side (kDa). $^*p<0.05$.

Cos-7 cells in comparison with Wt cells (Fig. 5c(i)).[20,21] The same results were obtained from the transient-transfectant NRCM (Supplementary Data Fig. 2c) and Cos-7 cells (data not shown) co-transfected with either Wt or E334K and EGFP and counted using flow cytometry (FACS) sorting for EGFP-positive cells. Staining with annexin V as shown in Fig. 5c(ii) supported the result that apoptosis was much higher in the E334K transfected cells in comparison with the Wt transfected cells.

Left ventricular dysfunction and dilation in patients carrying the E334K mutation

Echocardiographic parameters were examined to investigate the relationship between the type of mutation and clinical data of the patients (Table 2). Patients carrying the E334K mutation were 52, 77, and 68 years old (average 65.7 years), those carrying another mutation were 69, 69, 74, 50 years (average 65.5 years), and control healthy subjects were 25 – 85 years (average 64.2 years). Patients carrying the E334K mutation had a significantly smaller ejection fraction (EF) and fraction shortening (FS), and significantly larger left ventricular end-diastolic diameter (LVEDd) in comparison with healthy subjects (Fig. 6). This fact was different with other patients carrying another mutation had a comparable EF and FS, and smaller or comparable LVEDd in comparison with the healthy subjects.

Discussion

In the present study, we initially identified five novel mutations and three novel polymorphisms in *MYBPC3* in Japanese patients with HCM (Table 1). Of the 30 HCM patients, seven (23.3%) carried *MYBPC3* mutations, which is in accord with the frequency of

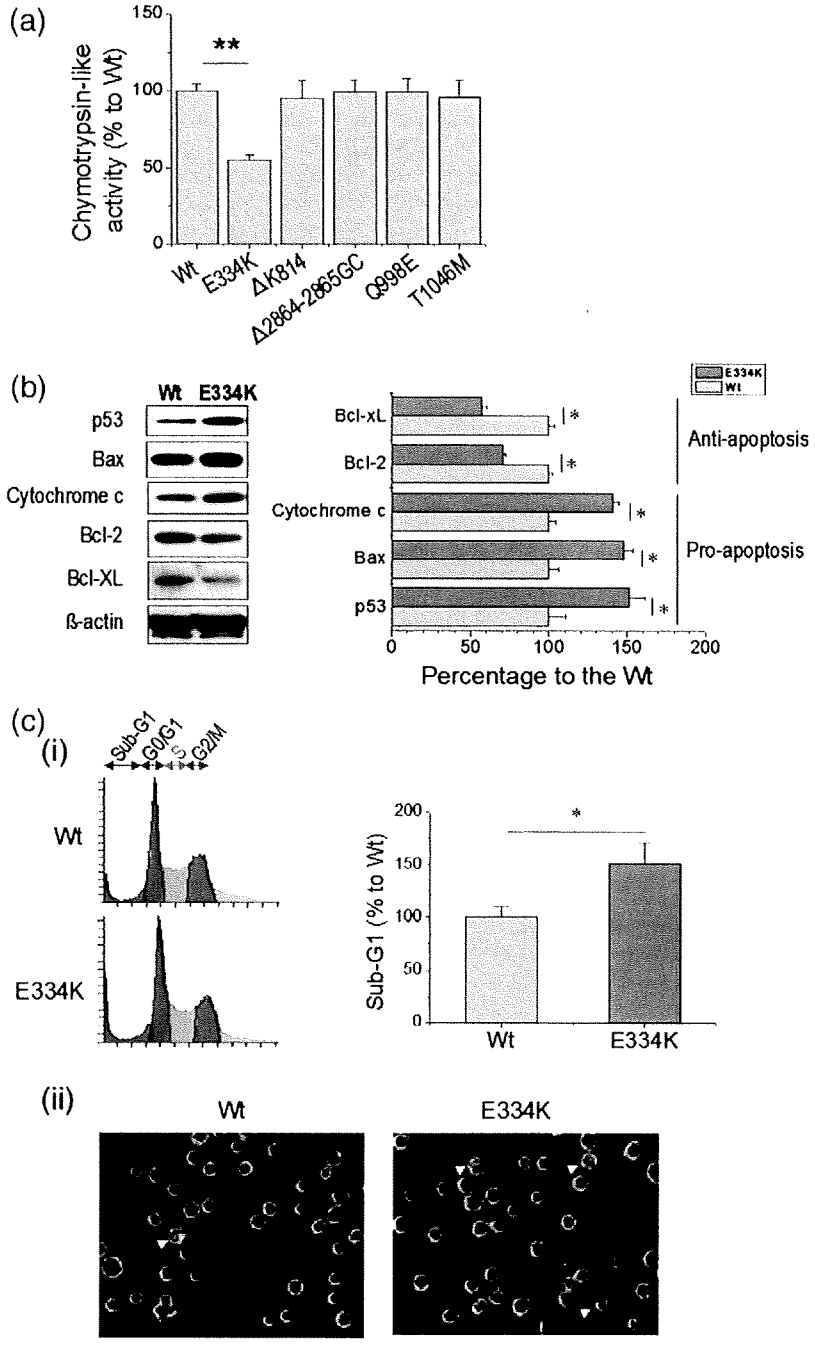

Fig. 5. Expression of E334K mutant cMyBP-C protein is associated with impaired UPS. (a) Measurement of 20 S proteasome activity (i.e. chymotrypsin-like activity). Purified proteasomes isolated from either Wt or other mutant myc-cMyBP-C stable transfectants of Cos-7 cells were prepared. The chymotrypsin-like activity was measured by detecting fluorescence of free 7-amino-4-methylcoumarin (AMC) liberated from a substrate peptide (Suc-Leu-Leu-Val-Tyr-AMC) digested specifically by this proteasome. $n = 7$. (b) Western blot analysis with anti-myc, anti-p53, anti-Bax, anti-cytochrome *c*, anti-Bcl-2, and anti-Bcl-xL detected the corresponding proteins in the either Wt or E334K mutant myc-cMyBP-C stable transfectants of Cos-7 cells. Left, representative Western blot; right, quantitative densitrometric scan of the indicated proteins in the stable E334K mutant myc-cMyBP-C transfectants of Cos-7 cells compared to the Wt, $n = 6$. (c(i)), FACS analysis of the cell population in the sub G-1 phase corresponding to apoptosis. Two hundred thousand of either Wt or E334K mutant myc-cMyBP-C stable transfectants of Cos-7 cells were analyzed with FACscan. Left, the representative plot of cell population in each cell cycle phase; right, the percentage of G-1 phase of stable E334K mutant myc-cMyBP-C transfectants of Cos-7 cells compared to the Wt, $n = 6$. (c(ii)), Wt or E334K mutant myc-cMyBP-C transfectants of Cos-7 cells were stained with annexin V and then visualized with a fluorescence microscope. $*p<0.05$, $**p<0.001$.

Table 2. Subject characteristics

No. subjects	Mutation	Average age (years)	Echocardiographic parameter				
			LVEDd (mm)	IVST (mm)	PWT (mm)	EF (%)	FS (%)
1	E334K	52	66	16	14	34.9	17
1	E334K	77	49.8	17	16	49	24.5
1	E334K	68	58.7	14	14	44	22.3
1	Δ814K	69	40	19	13	68	38.3
1	Δ2864-2865GC	69	45	20	17	62	33.3
1	Q998E	74	31.4	13.6	10.5	74	42
1	T1046M	50	41	31.4	21	76	43.9
40	Normal	64.2 (25–85)	46.8	9.1	9.1	68.3	38

18.5-42% reported earlier.[2–4] Of the five novel mutations, two were deletions and three were missense mutations. A deletion of two bases at exon 27 (Δ2864-2865GC) causes a frame-shift and a STOP codon, and results in the loss of the terminal 332 amino acid residues, which are replaced by 125 novel residues. Other mutations were ΔK814, E334K, Q998E, and T1046M.

We found that the level of E334K mutant protein was remarkably reduced in transfected COS7 cells as well as NRCM in comparison with the Wt and other mutant cMyBP-Cs (Fig. 2a; Supplementary Data Fig. 1a), regardless of the comparable level of transcription among them (Fig. 2b and Supplementary Data Fig. 1c). E334K mutant protein had a significantly shorter half-life (Fig. 3) with a higher level of polyubiquitination than the Wt (Fig. 2d), resulting in a decreased steady-state level of the protein. MG132 treatment (50 μM, 6 h) rescued its expression (Fig. 2c and Supplementary Data Fig. 1a) to a level comparable with that of Wt protein, indicating that degradation by the UPS accounts for the instability of E334K mutant cMyBP-C. This is the first evidence that a missense *MYBPC3* mutation found in patients with HCM causes instability of cMyBP-C, although the truncated cMyBP-C has been known to be degraded through the UPS. The missense mutation of E334K is located at exon 12, which is part of the coding region of the MyBP-C motif located in the N-terminus between C1 and C2, and has a regulatory function.[17] Although this region includes its phosphorylation site, there was no difference in phosphorylation between the E334K mutant and Wt cMyBP-Cs (Fig. 4c). On the other hand, a substitution of the negatively charged glutamic acid by the differently charged residue in this region influenced the level of protein expression (Fig. 4a), suggesting that protein stability is amino acid charge-dependent, which is supported by a previous report showing that substitution of amino acid to the charged residue in cMyBP-C was responsible for the thermodynamic stability of the unfolded protein.[19] As shown in Fig. 2a, the change of protein expression was not found on the other identified mutants: ΔK814 caused loss of a negatively charged amino acid (−1); Δ2864-2865GC caused loss of the terminal 332 amino acid residues, which are replaced by 125 novel residues; Q998E caused an amino acid charge change of −1; and T1046M caused no change of amino acid charge. One possible explanation is that

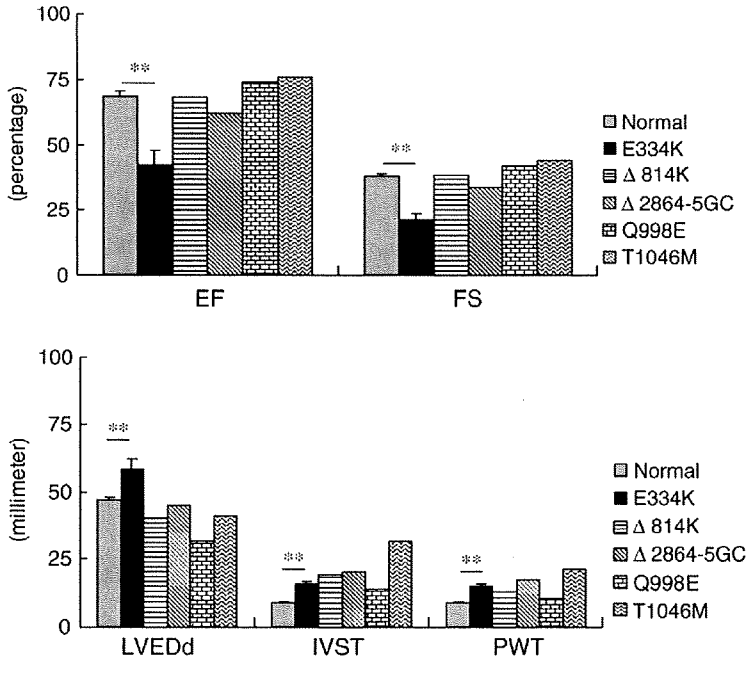

Fig. 6. Left ventricular dysfunction and dilation in patients carrying the E334K mutation. Echocardiographic data of patients carrying the E334K mutation (E334K, $n=3$) compared to the healthy subjects (Normal, $n=40$), and patients carrying other mutations of *MYBPC3*. The upper panel shows ejection fraction (EF) and fraction shortening (FS); the lower panel shows left ventricular end-diastolic diameter (LVEDd), interventricular septal wall thickness (IVST), and left ventricular posterior wall thickness (PWT). $*p<0.05$, $**p<0.001$.

the protein stability is influenced by the type of mutation in the gene, and its position.[19] Therefore, we think that the substitution of glutamic acid for a differently charged residue in certain positions would relate to the impaired protein structure and stability of cMyBP-C; however, we could not analyze the effect of E334K mutation on its protein structure directly because of lack of information on the crystal structure of cMyBP-C boundary amino acid at 334. This warrants further investigation.

The most prominent finding in the present study was that expression of the E334K mutant cMyBP-C caused UPS impairment characterized by decreased level of 20 S proteasome activity, increased the ratio of proapoptotic/antiapoptotic regulating protein, and increased apoptosis (Fig. 5 and Supplementary Data Fig. 2), although the other mutant cMyBP-Cs identified in this study did not induce UPS impairment (Fig. 5a and Supplementary Data Fig. 2a). UPS is a well-known internal pathway of cells meant to degrade unfolded or misfolded protein, and UPS impairment leads to cell apoptosis. Evidence of UPS impairment has been documented in the failing heart of a mouse model of pressure-overloaded heart. Apoptosis of cardiomyocytes was observed along with reduced proteasome activity and elevation of the ratio of proapoptotic/antiapoptotic protein in failing hearts.[16] Sarikas *et al.* recently reported that UPS impairment was a consequence of its encounter with truncated cMyBP-C.[15] This was the first report that a missense *MYBPC3* mutation can induce UPS impairment. As expected, three unrelated HCM patients carrying the E334K mutant *MYBPC3* developed left ventricular dysfunction and dilation (Fig. 6). Thus, cardiac dysfunction in these patients with HCM may be related to the rapid degradation of E334K mutant cMyBP-C through UPS to induce cMyBP-C instability.

The limitation of this study was that a direct link between experimental findings and the clinical phenotype observed in the patients could not be analyzed, since the cardiac biopsy tissue was not available. Another way to identify the link is by performing an *in vivo* study using an animal model and then checking the mutation effect on both physiological and molecular biological aspects. This warrants further investigation.

In conclusion, our results show that the missense *MYBPC3* mutation E334K destabilizes its protein through UPS and may contribute to cardiac dysfunction in HCM through UPS impairment.

Materials and Methods

Identification of *MYBPC3* mutations

The subjects were 30 Japanese patients diagnosed at Tottori University Hospital as having primary hypertrophic cardiomyopathy. Briefly, clinical diagnostic criteria were defined in adults by a maximum wall thickness>13 mm on echocardiography in the absence of another confounding diagnosis. Genomic DNA was extracted from peripheral white blood cells using a standard phenol/chloroform procedure. PCR primers were designed according to the published genomic sequences of *MYBPC3*.[10] All exons and flanking sequences of *MYBPC3* were screened for mutations using denaturing HPLC (Transgenomic WAVE® System, Omaha, NE), and each abnormal pattern was confirmed by direct sequencing (Abi Prism® 373 DNA Sequencer, Applied Biosystems, Foster City, CA). A cohort of 100 unrelated healthy individuals served as negative controls. Informed consent for participation in this study was obtained. The investigation conformed to the principles outlined in the Declaration of Helsinki.[22]

Clinical characterization

The evaluation of probands included medical history, clinical examination, biochemical markers, 12-lead electrocardiography, X-ray, and echocardiography.

Construction and expression of plasmid and generation of stable transfected cell

cDNA encoding Wt cMyBP-C was ligated into pcDNA3.1(+)-6myc with suitable restriction enzyme recognition sites (EcoRI and XhoI) to generate the expression vectors encoding the 6-myc epitope of the amino terminus of Wt cDNA.[13] cDNAs carrying five different novel mutations (Table 1) were generated by PCR mutagenesis (Stratagene, La Jolla, CA) in the Wt cDNA with two complementary overlapping primers (Table 3). Three cDNAs encoding myc-cMyBP-Cs with different electrical charges of the amino acid at position 334 were generated using the primers given in Table 3 in addition to the Wt/glutamic acid (E, negative charge) and lysine (K, positive charge). They were aspartic acid (D, negative charge), glutamine (Q, uncharged), and glycine (G, nonpolar). COS-7 cells were maintained in Dulbecco's modified Eagle's medium (DMEM, Wako, Osaka, Japan) supplemented with 10% (v/v) fetal bovine serum (Gibco, Invitrogen) and 0.5% (w/v) penicillin-streptomycin G (Wako) at 37 °C in a 5% CO_2 incubator. Cells were transfected using lipofectamine (Invitrogen) in accordance with the manufacturer's recommendations. Cells were assayed at 48–72 h after transfection. Proteasome inhibitors, lactacystine, proteasome inhibitor 1 and MG132 were dissolved in DMSO and added 6 h before the assays.[23] The final concentration of DMSO in the culture medium was ≤0.01% (v/v).

Generation of stable myc-cMyBP-C transfectants of Cos-7 cells was done by transfection and selection of clones with 1 mg/mL of geneticin (Wako, Osaka, Japan). Positive clones were expanded, passaged several times, and analyzed.

Western blotting and immunoprecipitation

Cells were scraped into lysis buffer (PBS containing 1% (v/v) NP40, 0.5% (w/v) sodium deoxycholate, 0.1% (w/v) SDS, 10 μg/mL aprotinin, 10 μg/mL leupeptin, 10 μg/mL pepstain, and 1 mM PMSF), lysed by sonication, and insoluble material was removed by centrifugation. The protein concentration was determined with a Protein Assay Kit (Bio-Rad). Proteins (10 μg each) were separated by SDS-PAGE and electrotransferred to a polyvinylidene difluoride (PVDF) membrane. Membranes were probed with antibodies against myc (Santa Cruz Biotechnology, Santa Cruz, CA), GFP (MBL, Nagoya, Japan), actin (Calbiochem, La Jolla, CA),

ubiquitin (MBL), phosphoserine (Chemicon International, Temecula, CA), p53 (Santa Cruz), Bax (Santa Cruz), cytochrome *c* (BD Biosciences, Franklin Lakes, NJ), and Bcl-2 (Santa Cruz), Bcl-xL (Santa Cruz), and were revealed using an ECL system (Amersham Bioscience, Piscataway, NJ). The band intensities were quantified using NIH image software. Immunoprecipitation was done in PBS containing 1% (v/v) Triton X-100, 0.5% SDS, 0.25% sodium deoxycholate, 1 mM EDTA, and protease inhibitors for 2 h at 4 °C. Immunocomplexes were collected with protein G/agarose (GE Healthcare, Uppsala, Sweden) and bound proteins were analyzed by SDS-PAGE followed by immunoblotting.

Real-time polymerase chain reaction (RT-PCR)

Total RNA from cultured cells was extracted using the RNeasy Plus Mini Kit (Qiagen, Valencia, CA) according to the manufacturer's instructions. RNA samples were treated with DNaseI (Promega) to eliminate genomic DNA contamination, and cDNA was synthesized using SuperScript™ II reverse transcriptase (Gibco-BRL). RT-PCR was done with the 7900HT Fast Real-Time PCR System, 384-well plate according to the manufacturer's instructions (Applied Biosystems, CA). The universal ProbeLybrary (Roche) probes #21 and #64 were used for MYBPC3 and β-actin, respectively. A MYBPC3 gene-specific primer set overlapping the end of exon 28 and the middle of exon 29 (forward 5′-ggtgctgcaggttgttgac-3′; reverse: 5′-acatcctggggtggcttc-3′) was used to obtain 102 bp products. The primers for β-actin overlapped the end of exon 3 and the middle of exon 4 (forward 5′-ccaaccgcgagaagatga-3′; reverse 5′-ccagaggcgtacagggatag-3′) resulting in 97 bp products. Data analysis was done with the SDS software version 3.2 (Applied Biosystems). cDNA was also amplified with PCR and separated by electrophoresis, stained with ethidium bromide and visualized in a UV transilluminator.

Pulse–chase analysis

Cells were pulse-labeled for 2 h in methionine-free DMEM supplemented with [^{35}S]methionine (3.7 Ci/mL, GE Healthcare) and then chased in DMEM supplemented with 1 mM methionine. Where indicated, proteasome inhibitors were included both in pulse and chase media. Anti-myc precipitation was carried out as described above and bound proteins were analyzed by SDS-PAGE followed by autoradiography. The band intensities were quantified using NIH image software. The decay constant (k) was estimated by fitting first-order decay curves to the form $y = e^{-kt}$, using SigmaPlot (Jandel Scientific, CA).[24] The half-life ($t_{1/2}$) was calculated as $t_{1/2} = \ln(2) / k$.

Flow cytometry analysis

Transfected cells were cultivated for 72 h. After treatment with trypsin, cells were harvested into a medium containing FBS, washed three times with PBS and centrifuged. The cell pellet was resuspended in PBS containing 0.1~0.2% Triton X-100 at approximately 1×10^5 cells/mL to obtain the nuclei. After pipetting several times, the cell suspension was filtered using a Cell Strainer (BD Falcon, Bedford, MA) to remove cell aggregates. RNase and propidium iodine were added, and cells were analyzed with a FACScan (Becton-Dickinson, San Jose, CA) flow cytometer up to 5×10^4cells. Data were analyzed using FLOWJO software (Becton-Dickinson).

Annexin V staining

Staining with annexin V was done with the Annexin V-PE Apoptosis Detection Kit Plus according to the manufacturer's instructions (MBL, Nagoya, Japan). Images were collected with a Nikon Eclipse TE2000-U fluorescence microscope.

Measurement of 20 S proteasome activity

Proteasomes were isolated using the Proteasome Isolation Kit (Calbiochem) according to the manufacturer's instruction, and resuspended in a buffer containing protease inhibitor. Using an assay kit (Calbiochem), 20 S proteasome (i.e., chymotrypsin-like) activity was measured. The reaction mixture contained 20 S proteasome (10 μg/mL) in the purified proteasome suspension, activation solution (0.03% SDS), substrate peptide (10 μM), and buffer (500 mM Hepes, 10 mM EDTA, pH 7.6). The mixture was incubated at 37 °C for 1 h. The substrate peptide (Suc-Leu-Leu-Val-Tyr-AMC) was digested by 20 S proteasome, liberating 7-amino-4-

Table 3. Primers for site-directed mutagenesis

Mutation		Sequence (5′ → 3′)
E334K	Forward	GCAGGCACCCCCATCTGAGTACAAGCGCATCGCCTTCCAGTACGG
	Reverse	CCGTACTGGAAGGCGATGCGCTTGTACTCAGATGGGGGTGCCTGC
ΔK814	Forward	CATCCTGGAGCGCAAGAAGAAGAGCTACCGGTGGATGCGGCTGA
	Reverse	TCAGCCGCATCCACCGGTAGCTCTTCTTCTTGCGCTCCAGGATC
Δ2864-2865GC	Forward	GCTGCTTTTCCGAGTGGGCACACAATATGG
	Reverse	CCATATTGTGTGCCCACTCGGAAAAGCAGC
Q998E	Forward	CTTCTCATCCCTTTCGAGGGCAAGCCCCGGC
	Reverse	GCCGGGGCTTGCCCTCGAAAGGGATGAGAAG
T1046M	Forward	GCACTTACCAGGTGATGGTGCGCATTGAGAA
	Reverse	TTCTCAATGCGCACCATCACCTGGTAAGTGC
E334K	Forward	GCAGGCACCCCCATCTGAGTACAAGCGCATCGCCTTCCAGTACGG
	Reverse	CCGTACTGGAAGGCGATGCGCTTGTACTCAGATGGGGGTGCCTGC
E334D	Forward	AGGCACCCCCATCTGAGTACGACCGCATCGCCTTCCAGTACGGCG
	Reverse	CGCCGTACTGGAAGGCGATGCGGTCGTACTCAGATGGGGGTGCCT
E334Q	Forward	GCAGGCACCCCCATCTGAGTACCAGCGCATCGCCTTCCAGTACGG
	Reverse	CCGTACTGGAAGGCGATGCGCTGGTACTCAGATGGGGGTGCCTGC
E334G	Forward	CAGGCACCCCCATCTGAGTACGGGCGCATCGCCTTCCAGTACGGC
	Reverse	GCCGTACTGGAAGGCGATGCGCCCGTACTCAGATGGGGGTGCCTG

methylcoumarin (AMC). The fluorescence of free AMC was detected in a fluorescence spectrometer (PerSeptive Biosystems Cytofluor II, Mountain View, CA; excitation 380 nm, emission 460 nm). Because the proteasome in this reaction is activated by SDS, the fluorescence liberated in the absence of SDS was taken as the background value (0%).

Statistical analysis

StatView for Windows software version 5 (SAS Institute Inc., Cary, NC) was used for the statistical analysis. Differences between two groups were assessed using Student's unpaired *t*-test, except for Fig. 6 which used the Mann-Whitney test. A two-way ANOVA with Fisher's exact test for post hoc analysis was used for multiple comparisons. All experimental data are expressed as mean±SEM. Differences with $p<0.05$ were considered statistically significant.

Acknowledgements

We thank Dr. Osamu Tsukamoto (Osaka University, Japan) for assistance with proteasome activity assay and Dr. Yasushi Kawata (Tottori University, Japan) for assistance with amino acid electrical charges analysis. This study was supported by a grant-in-aid for Scientific Research from the Ministry of Education, Culture, Sports, Science and Technology (MEXT) of Japan (18590775) (to I.H.), and by the sixth Framework Program of the European Union (Marie Curie EXT-014051) and the Deutsche Forschungsgemeinschaft (FOR-604/1, CA 618/1-1) (to L.C.). U.B was supported as a Japanese Government Research Scholarship from the MEXT.

Supplementary Data

Supplementary data associated with this article can be found, in the online version, at doi:10.1016/j.jmb.2008.09.070

References

1. Seidman, J. G. & Seidman, C. (2001). The genetic basis for cardiomyopathy: from mutation identification to mechanistic paradigms. *Cell*, **104**, 557–567.
2. Richard, P., Villard, E., Charron, P. & Isnard, R. (2006). The genetic bases of cardiomyopathies. *J. Am. Coll. Cardiol.* **48**, A79–A89.
3. Erdmann, J., Daehmlow, S., Wischke, S., Senyuva, M., Werner, U., Raible, J. *et al.* (2003). Mutation spectrum in a large cohort of unrelated consecutive patients with hypertrophic cardiomyopathy. *Clin. Genet.* **64**, 339–349.
4. Richard, P., Charron, P., Carrier, L., Ledeuil, C., Cheav, T., Pichereau, C. *et al.* (2003). Hypertrophic cardiomyopathy: distribution of disease genes, spectrum of mutations, and implications for a molecular diagnosis strategy. *Circulation*, **107**, 2227–2232.
5. Mörner, S., Richard, P., Kazzam, E., Hellman, U., Hainque, B., Schwartz, K. *et al.* (2003). Identification of the genotypes causing hypertrophic cardiomyopathy in northern Sweden. *J. Mol. Cell. Cardiol.* **35**, 841–849.
6. Jääskeläinen, P., Kuusisto, J., Miettinen, R., Kärkkäinen, P., Kärkkäinen, S., Heikkinen, S. *et al.* (2002). Mutations in the cardiac myosin-binding protein C gene are the predominant cause of familial hypertrophic cardiomyopathy in eastern Finland. *J. Mol. Med.* **80**, 412–422.
7. Winegrad, S. (1999). Cardiac myosin binding protein C. *Circ. Res.* **84**, 1117–1126.
8. McClellan, G., Kulikovskaya, I. & Winegrad, S. (2001). Changes in cardiac contractility related to calcium-mediated changes in phosphorylation of myosin-binding protein C. *Biophys. J.* **81**, 1083–1092.
9. Bonne, G., Carrier, L., Bercovici, J., Cruaud, C., Richard, P. & Hainque, B. (1995). Cardiac myosin binding protein-C gene splice acceptor site mutation is associated with familial hypertrophic cardiomyopathy. *Nat. Genet.* **11**, 438–440.
10. Carrier, L., Bonne, G., Bahrend, E., Yu, B., Richard, P. & Niel, F. (1997). Organization and sequence of human cardiac myosin binding protein C gene *(MYBPC3)* and identification of mutations predicted to produce truncated proteins in familial hypertrophic cardiomyopathy. *Circ. Res.* **80**, 427–434.
11. Rottbauer, W., Gautel, M., Zehelein, J., Labeit, S., Franz, W. M. & Fischer, C. (1997). Novel splice donor site mutation in the cardiac myosin-binding protein-C gene in familial hypertrophic cardiomyopathy. Characterization of cardiac transcript and protein. *J. Clin. Invest.* **100**, 475–482.
12. Moolman, J. A., Reith, S., Uhl, K., Bailey, S., Gautel, M. & Jeschke, B. (2000). A newly created splice donor site in exon 25 of the MyBP-C gene is responsible for inherited hypertrophic cardiomyopathy with incomplete disease penetrance. *Circulation*, **101**, 1396–1402.
13. Flavigny, J., Souchet, M., Sébillon, P., Bailey, S., Gautel, M., Jeschke, B. *et al.* (1999). COOH-terminal truncated cardiac myosin-binding protein C mutants resulting from familial hypertrophic cardiomyopathy mutations exhibit altered expression and/or incorporation in fetal rat cardiomyocytes. *J. Mol. Biol.* **294**, 443–456.
14. Yang, Q., Sanbe, A., Osinska, H., Hewett, T. E., Klevitsky, R. & Robbins, J. (1999). In vivo modeling of myosin binding protein C familial hypertrophic cardiomyopathy. *Circ. Res.* **85**, 841–847.
15. Sarikas, A., Carrier, L., Schenke, C., Doll, D., Flavigny, J., Lindenberg, K. S. *et al.* (2005). Impairment of the ubiquitin-proteasome system by truncated cardiac myosin binding protein C mutants. *Cardiovasc. Res.* **66**, 33–44.
16. Tsukamoto, O., Minamino, T., Okada, K., Shintani, Y., Takashima, S. & Kato, H. (2006). Depression of proteasome activities during the progression of cardiac dysfunction in pressure-overloaded heart of mice. *Biochem. Biophys. Res. Commun.* **340**, 1125–1133.
17. Gautel, M., Zuffardi, O., Freiburg, A. & Labeit, S. (1995). Phosphorylation switches specific for the cardiac isoform of myosin binding protein-C: a modulator of cardiac contraction? *EMBO J.* **14**, 1952–1960.
18. Kulikovskaya, I., McClellan, G., Flavigny, J., Carrier, L. & Winegrad, S. (2003). Effect of MyBP-C binding to actin on contractility in heart muscle. *J. Gen. Physiol.* **122**, 761–774.
19. Idowu, S. M., Gautel, M., Perkins, S. J. & Pfuhl, M. (2003). Structure, stability and dynamics of the central

domain of cardiac myosin binding protein C (MyBP-C): implications for multidomain assembly and causes for cardiomyopathy. *J. Mol. Biol.* **329**, 745–761.
20. Schmid, I., Uittenbogaart, C. H. & Giorgi, J. V. (1994). Sensitive method for measuring apoptosis and cell surface phenotype in human thymocytes by flow cytometry. *Cytometry*, **15**, 12–20.
21. Nomura, M., Nomura, N., Newcomb, E. W., Lukyanov, Y., Tamasdan, C. & Zagzag, D. (2004). Geldanamycin induces mitotic catastrophe and subsequent apoptosis in human glioma cells. *J. Cell. Physiol.* **201**, 374–384.
22. World Medical Association Declaration of Helsinki. (1997). Recommendations guiding physicians in biomedical research involving human subjects. *Cardiovasc. Res.* **35**, 2–3.
23. Lee, D. H. & Goldberg, A. L (1998). Proteasome inhibitors: valuable new tools for cell biologists. *Trends Cell. Biol.* **8**, 397–403.
24. Kato, M., Ogura, K., Miake, J., Sasaki, N., Taniguchi, S., Igawa, O. *et al.* (2005). Evidence for proteasomal degradation of Kv1.5 channel protein. *Biochem. Biophys. Res. Commun.* **337**, 343–348.

虚血性心筋障害に対するエリスロポエチンの保護効果

Erythropoietin exerts cardioprotective effects against ischemic insults

南野哲男
Tetsuo MINAMINO
大阪大学大学院医学系研究科循環器内科学

◎心筋梗塞患者の予後改善のためには，心筋梗塞サイズを縮小し，梗塞後心室リモデリングを抑制する必要がある．動物実験にてエリスロポエチン(EPO)はいずれの過程にも作用し，心臓保護効果を呈することが示されている．さらに興味深いことに，EPOの心保護効果は再灌流時投与においても認められることから，臨床応用への期待が大きい．本稿では著者らのデータも含めて，虚血性心筋障害に対するEPOの心保護メカニズムについて述べたい．さらに，現在進行中であるEPOを用いた臨床試験についても紹介したい．

Key word：エリスロポエチン(EPO)，急性心筋梗塞，心室リモデリング，血管内皮前駆細胞，RISK pathway

急性心筋梗塞はいぜん死亡率の高い疾患であり，また，梗塞後心不全は“生活の質の低下”や医療費増大を招くため，心筋梗塞への取組みは循環器医にとって重要な課題である．急性期心筋梗塞治療として，心筋梗塞サイズ縮小を目的とした経皮経管冠動脈形成術などの再灌流療法が施行される．また，慢性期治療としては心臓リモデリング抑制を目的としたレニン-アンジオテンシン系阻害薬やβ遮断薬による内科的治療が行われる．これらの治療戦略は一定の成果を残しつつも，梗塞後心不全をきたす症例は増加する傾向にある．そのため，急性心筋梗塞に対するあらたな治療法の開発が期待されている．

近年，動物実験において，造血サイトカインであるエリスロポエチン(EPO)が心筋梗塞サイズを縮小し，左室リモデリングを抑制することが報告されており，注目されている．また，これらの心保護効果は再灌流時投与においても認められることから，臨床への応用が期待されている．

EPOの心臓保護効果

腎性貧血治療薬として広く臨床応用されているEPOは，赤芽球系細胞の増殖・分化の促進作用ならびにアポトーシス抑制作用を有している[1]．興味深いことに，EPO受容体は赤芽球系細胞のみな

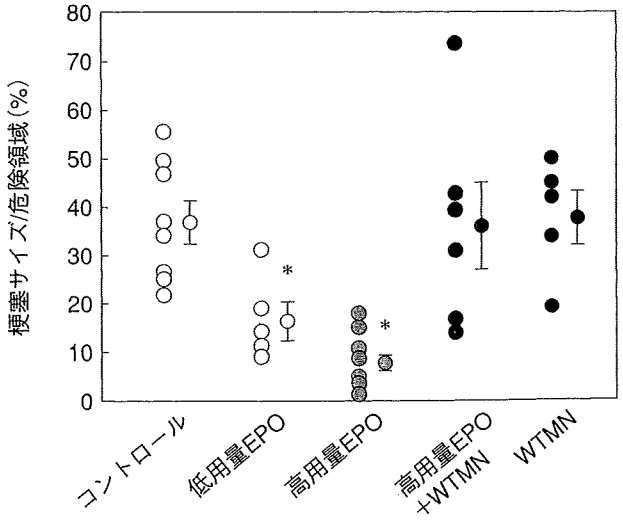

図1　EPOによる急性期心筋梗塞サイズ縮小結果[2]
EPOは用量依存性に梗塞サイズを縮小する．
*：$p<0.05$ vs. コントロール．

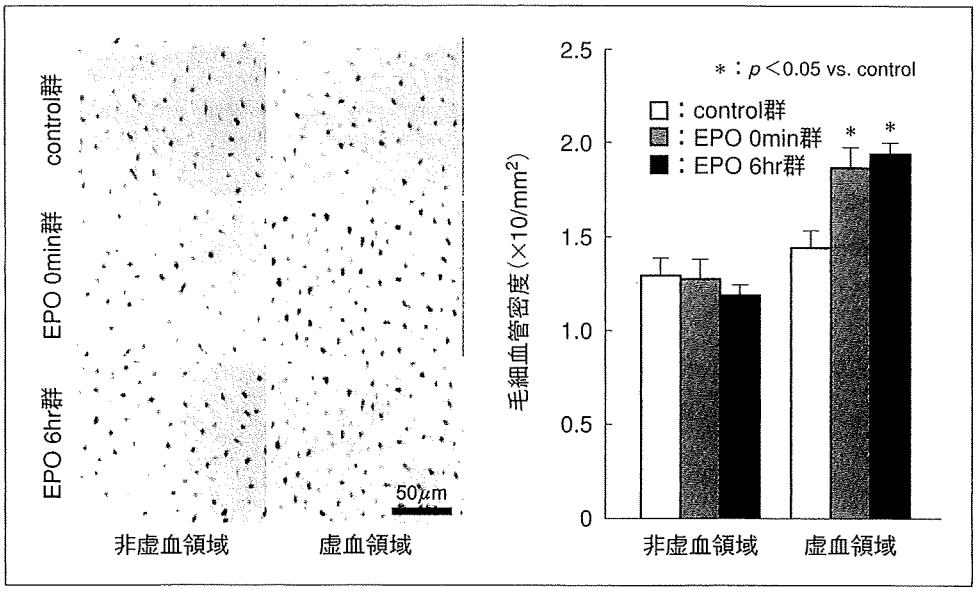

図 2　EPO による虚血領域における毛細血管数の増加[3)]
左：組織染色像(von Will brand 因子)，右：定量データ．

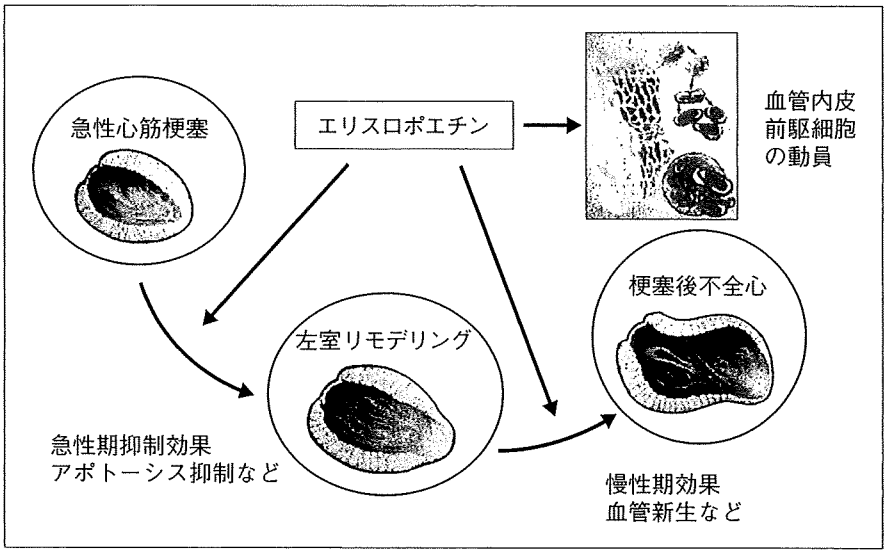

図 3　EPOの虚血心筋保護作用

らず心筋細胞や血管内皮細胞にも存在することが明らかになった．さらに近年，EPO が血管内皮前駆細胞(EPC)増加作用を有することが報告された[1)]．近年，EPO がアポトーシス抑制を介して心筋梗塞サイズを縮小すること，ならびに，EPC 増加による血管新生促進を介して梗塞後心臓リモデリングを抑制することが報告されている[2,3)]．

1．EPOの心筋梗塞サイズ縮小効果

著者らは麻酔開胸犬を用いて，90 分虚血・6 時間再灌流による心筋梗塞モデルを作成した．再灌流直前に静脈内単回投与した EPO は濃度依存性に心筋梗塞サイズを縮小すること，ならびに EPO による心筋梗塞サイズ縮小効果は PI3 キナーゼ阻害剤である Wortmannin(WTMN)にて抑制されることを報告した(図 1)[2)]．このとき，虚血領域における TUNEL 陽性細胞数は EPO 投与により減少したが，WTMN 投与によりその抑制効果は消失した．これらのことから，EPO の再灌流時投与は PI3K を介してアポトーシスを抑制し，心筋梗塞サイズを縮小することが明らかになった．EPO による急性心筋梗塞サイズ縮小効果にはアポトーシス抑制以外にもラジカルスカベンジャー作用や抗炎

症作用などのEPOの多様な心保護作用も関与していると考えられている[1].

2. EPOの梗塞後心臓リモデリング抑制効果

つぎに著者らは，麻酔開胸犬を用いて心筋梗塞による慢性心不全モデルを作成した[3]．梗塞後1週間ではコントロール群で比べ，EPO投与群ではEPCの指標である末梢血中CD34陽性単核球数ならびに虚血領域における毛細血管数の増加が認められた(図2)．再灌流直後EPO投与群のみならず6時間後EPO投与群においても，梗塞作成後4週間の左室駆出率はコントロール群と比較して高値を示した．EPO投与群では毛細血管数が増加し虚血領域への血流量が増大するため，慢性期心臓リモデリングを抑制した可能性が示された．また，梗塞作成後24時間でのEPO投与でも心筋梗塞サイズを縮小することや，長期間作用型EPOの梗塞後慢性投与(週1回の割合で3週間)でも心機能改善が認められることが報告されている[1]．梗塞後心臓リモデリング抑制効果を目的としたEPOの最適な投与方法についての検討が続いている．

以上より，虚血性心筋障害に対するエリスロポエチンの保護効果は異なったメカニズムを介していると考えられる(図3)．

EPOの細胞内情報伝達

近年，再灌流開始後に生じる心筋細胞障害を抑制するポストコンディショニング現象が注目されている[4]．本現象は長時間虚血後再灌流時に冠動脈血流を間欠的に回復させることにより心筋梗塞サイズが縮小するものである．このポストコンディショニングをつかさどる細胞内情報伝達経路として，reperfusion injury salvage kinase(RISK)pathwayが重要である[5]．RISK pathwayは複数の細胞内シグナル伝達経路から構成されており，MAPキナーゼ系，JAK/STAT系，PI3K/AKT系が中心である．EPOは心筋細胞や血管内皮細胞上に存在するEPO受容体を介して，RISK pathwayのメンバーを活性化することが明らかになっている．これまで著者らの報告も含めて，PI3KがEPOによる心筋梗塞サイズ縮小効果に中心的な役割を果たすことを示唆するものが多い[1,3]．

臨床応用

これまでの小規模臨床試験において冠血管インターベンション直前の長期作用型EPOまたはEPO単回投与では明らかな副作用の増加はなかったものの，心筋梗塞サイズ縮小効果も認められないことが報告されている[6,7]．現在，急性心筋梗塞患者466例を対象にEPO(60,000単位)投与の6週間後左駆出率に及ぼす影響を検討する臨床試験が進行中であり，その結果が待たれる[8]．

おわりに

過去5年間，動物実験モデルにおいてEPOの心筋梗塞サイズ縮小効果ならびに梗塞後心室リモデリング抑制効果が数多く報告されている．今後，EPOの急性期心筋梗塞を対象とした臨床試験の実施ならびにその成果報告が待たれる．

文献

1) Riksen, N. P. et al.：Erythropoietin：ready for prime-time cardioprotection. *Trends Pharmacol. Sci.*, **29**：258-267, 2008.
2) Hirata, A. et al.：Erythropoietin just before reperfusion reduces both lethal arrhythmias and infarct size via the phosphatidylinositol-3 kinase-dependent pathway in canine hearts. *Cardiovasc. Drugs Ther.*, **19**：33-40, 2005.
3) Hirata, A. et al.：Erythropoietin enhances neovascularization of ischemic myocardium and improves left ventricular dysfunction after myocardial infarction in dogs. *J. Am. Coll. Cardiol.*, **48**：176-184, 2006.
4) Zhao, Z. Q. and Vinten-Johansen, J.：Postconditioning：reduction of reperfusion-induced injury. *Cardiovasc. Res.*, **70**：200-211, 2006. [Epub 2006 Mar. 20].
5) Hausenloy, D. J. et al.：The reperfusion injury salvage kinase pathway：a common target for both ischemic preconditioning and postconditioning. *Trends Cardiovasc. Med.*, **15**：69-75, 2005.
6) Lipsic, E. et al.：A single bolus of a long-acting erythropoietin analogue darbepoetin alfa in patients with acute myocardial infarction：a randomized feasibility and safety study. *Cardiovasc. Drugs Ther.*, **20**：135-141, 2006.
7) Liem, A. et al.：Effect of EPO administration on myocardial infarct size in patients with non-STE acute coronary syndromes：results from a pilot study. *Int. J. Cardiol.*, 2007. [Epub ahead of print]
8) Belonje, A. M. et al.：Effects of erythropoietin after an acute myocardial infarction：rationale and study design of a prospective, randomized, clinical trial(HEBEⅢ). *Am. Heart J.*, **155**：817-822, 2008.

Journal of Molecular and Cellular Cardiology 46 (2009) 452–462

Contents lists available at ScienceDirect

Journal of Molecular and Cellular Cardiology

journal homepage: www.elsevier.com/locate/yjmcc

Original article

PKA rapidly enhances proteasome assembly and activity in in vivo canine hearts

Mitsutoshi Asai [a], Osamu Tsukamoto [a,b], Tetsuo Minamino [a,*], Hiroshi Asanuma [b], Masashi Fujita [a], Yoshihiro Asano [a], Hiroyuki Takahama [b], Hideyuki Sasaki [b], Shuichiro Higo [a], Masanori Asakura [b], Seiji Takashima [a], Masatsugu Hori [c], Masafumi Kitakaze [b]

[a] Department of Cardiovascular Medicine, Osaka University Graduate School of Medicine, Suita, 565-0871, Japan
[b] Department of Cardiovascular Medicine, National Cardiovascular Center, Suita 565-8565, Japan
[c] Osaka Medical Center for Cancer and Cardiovascular Diseases, Osaka 537-8511, Osaka, Japan

ARTICLE INFO

Article history:
Received 14 July 2008
Received in revised form 16 October 2008
Accepted 3 November 2008
Available online 13 November 2008

Keywords:
Proteasome
PKA
Phosphorylation
Assembly
Ubiquitinated protein
Ischemia/reperfusion

ABSTRACT

Proteasome regulates diverse cellular functions by eliminating ubiquitinated proteins. Protein kinase A (PKA) is a key regulator of proteasome activity. However, it remains unknown how PKA regulates proteasome activity and whether it controls proteasome activity in in vivo hearts. Both the in vitro peptidase assay and the in-gel peptidase assays showed that the treatment with PKA for 30 min dose-dependently activated purified 26S proteasome. Simultaneously, PKA treatment enhanced phosphorylation and assembly of purified 26S proteasome evaluated by non-reducing native polyacrylamide gel electrophoresis, either of which was blunted by the pretreatment with a PKA inhibitor, H-89. In in vivo canine hearts, proteasome assembly and activity were enhanced 30 min after the exogenous or endogenous stimulation of PKA by the intracoronary administration of isoproterenol or forskolin for 30 min or by ischemic preconditioning (IP) with 4 times of repeated 5 min of ischemia. The intracoronary administration of H-89 blunted the enhancement of proteasome assembly and activity by IP. Myocardial proteasome activity at the end of ischemia was decreased compared with the control, however, it did not differ from the control in dogs with IP. IP decreased the accumulation of ubiquitinated proteins in the canine ischemia/reperfusion myocardium, which was blunted by the intracoronary administration of a proteasome inhibitor, epoxomicin. However, proteasome activation by IP was not involved in its infarct size-limiting effects. These findings indicate that PKA rapidly enhances proteasome assembly and activity in in vivo hearts. Further investigation will be needed to clarify pathophysiological roles of PKA-mediated proteasome activation in ischemia/reperfusion hearts.

1. Introduction

The ubiquitin–proteasome system plays a major role in intracellular protein degradation and subsequently regulates cellular functions in various cells [1–4]. 26S proteasome is composed of 20S proteasome as its "core" catalytic unit capped on each end by 19S regulatory complex [5,6]. 26S proteasome is a cylinder-like structure containing 4 concentric rings, each containing 7 subunits. We have previously reported that impairment of proteasome activity may contribute to the progression of cardiac dysfunction along with the accumulation of ubiquitinated proteins in the pressure-overloaded heart of mice [7]. In addition, Bulteau et al. clearly demonstrated the deactivation of proteasome and the subsequent accumulation of ubiquitinated proteins in ischemia/reperfusion myocardium [8]. These findings suggest that impairment of the ubiquitin–proteasome system may be closely associated with cardiac diseases. Therefore, a better understanding the regulation of the ubiquitin–proteasome system may lead to new therapies for cardiac diseases. However, it remains largely unknown how proteasome is regulated in in vivo hearts.

There are several possible mechanisms that could regulate 26S proteasome activity, including 1) changes in protein levels of proteasome subunits, 2) post-translational modification of proteasome subunit such as phosphorylation/dephosphorylation, and 3) assembly/disassembly of proteasome subunits [9,10]. Recently, protein kinase A (PKA) is reported to be one of the key regulators of proteasome activity in the in vitro studies [11,12]. PKA increases proteolytic activities of the cardiac proteasome [11] and phosphorylation of the 19S proteasome subunit by PKA correlates with increased proteasome activity [12]. However, it remains to be resolved whether PKA increases proteasome activity by altering the status of proteasome assembly or by phosphorylating proteasome subunits. Thus, in the present study, we first investigated phosphorylation, assembly and activity of purified proteasome when it was treated with PKA. Next, we investigated proteasome assembly and activity in in vivo canine hearts when cardiac PKA was stimulated endogenously and

* Corresponding author. Tel.: +81 6 6879 3635; fax: +81 6 6879 3473.
E-mail address: minamino@medone.med.osaka-u.ac.jp (T. Minamino).

0022-2828/$ – see front matter © 2008 Elsevier Inc. All rights reserved.
doi:10.1016/j.yjmcc.2008.11.001

exogenously. We also checked the time-course changes in proteasome activity during ischemia/reperfusion period in dogs with and without endogenous PKA stimulation. Finally, we investigated the role of PKA-mediated proteasome activation by IP in the accumulation of ubiquitinated proteins and myocardial infarct size using a proteasome inhibitor.

2. Methods

2.1. Materials

Epoxomicin (a proteasome inhibitor), PKA, isoproterenol, forskolin and 2,3,5-triphenyltetrazolium chloride (TTC) were obtained from Sigma (St. Louis, MO, USA). A purified 26S proteasome from human erythrocyte and Suc-Leu-Leu-Val-Tyr-7-amino-4-methylcoumarin (proteasome peptidase substrates) were obtained from Biomol International (Plymouth Meeting, PA, USA). H-89 (a selective PKA inhibitor) and an antibody against serine/threonine phosphorylated proteins were obtained from Upstate (Lake Placid, NY, USA). Antibodies directed against ubiquitinated proteins (clone FK2) and proteasome subunits (Rpt5, α7, and β5) were purchased from Biomol International. Clone FK2 recognizes both mono- and poly-ubiquitinated proteins but not free ubiquitin, so the extent of protein ubiquitination could be determined.

2.2. Measurement of 26S proteasome activity

2.2.1. In vitro peptidase assay

The purified erythrocyte 26S proteasomes treated with various units of PKA with and without 100 μmol/L H-89

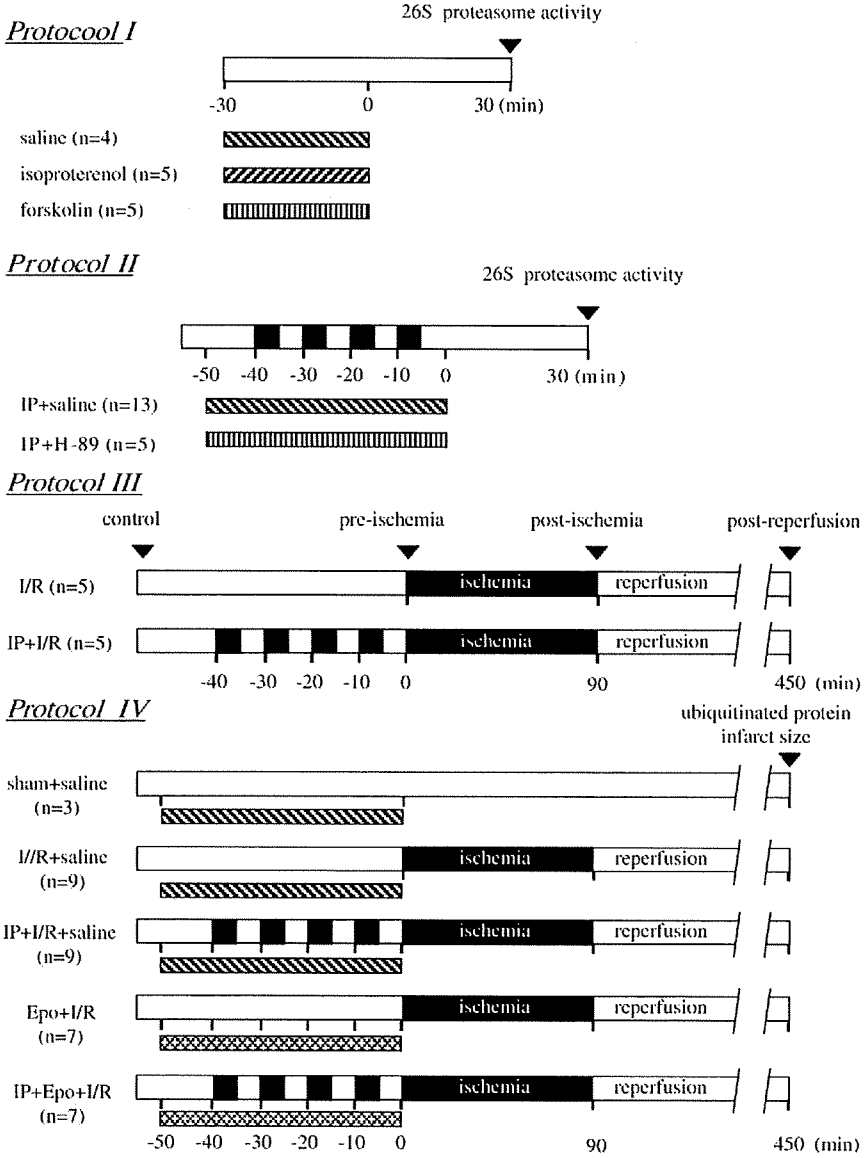

Fig. 1. Experimental protocols in canine model. (Protocol I) Effects of the intracoronary administration of saline ($n=4$), isoproterenol ($n=5$) or forskolin ($n=5$) (an exogenous stimulant of PKA) on proteasome activity in canine hearts. (Protocol II) Effects of ischemic preconditioning (IP) (an endogenous stimulant of PKA) with the intracoronary administration of saline ($n=8$ in LAD-perfused myocardium and $n=5$ in LCx-perfused one) or H-89 ($n=5$) (a PKA inhibitor) on proteasome activity in canine hearts. (Protocol III) Time-course changes in proteasome activity during ischemia/reperfusion period with and without IP ($n=5$ per each group). The triangle indicates the timing for myocardial biopsy. (Protocol IV) Effects of proteasome activation by IP on the accumulation of ubiquitinated proteins and infarct size in canine hearts. Sham operation was performed in 3 dogs. I/R and Epo indicate ischemia/reperfusion and epoxomicin, respectively.

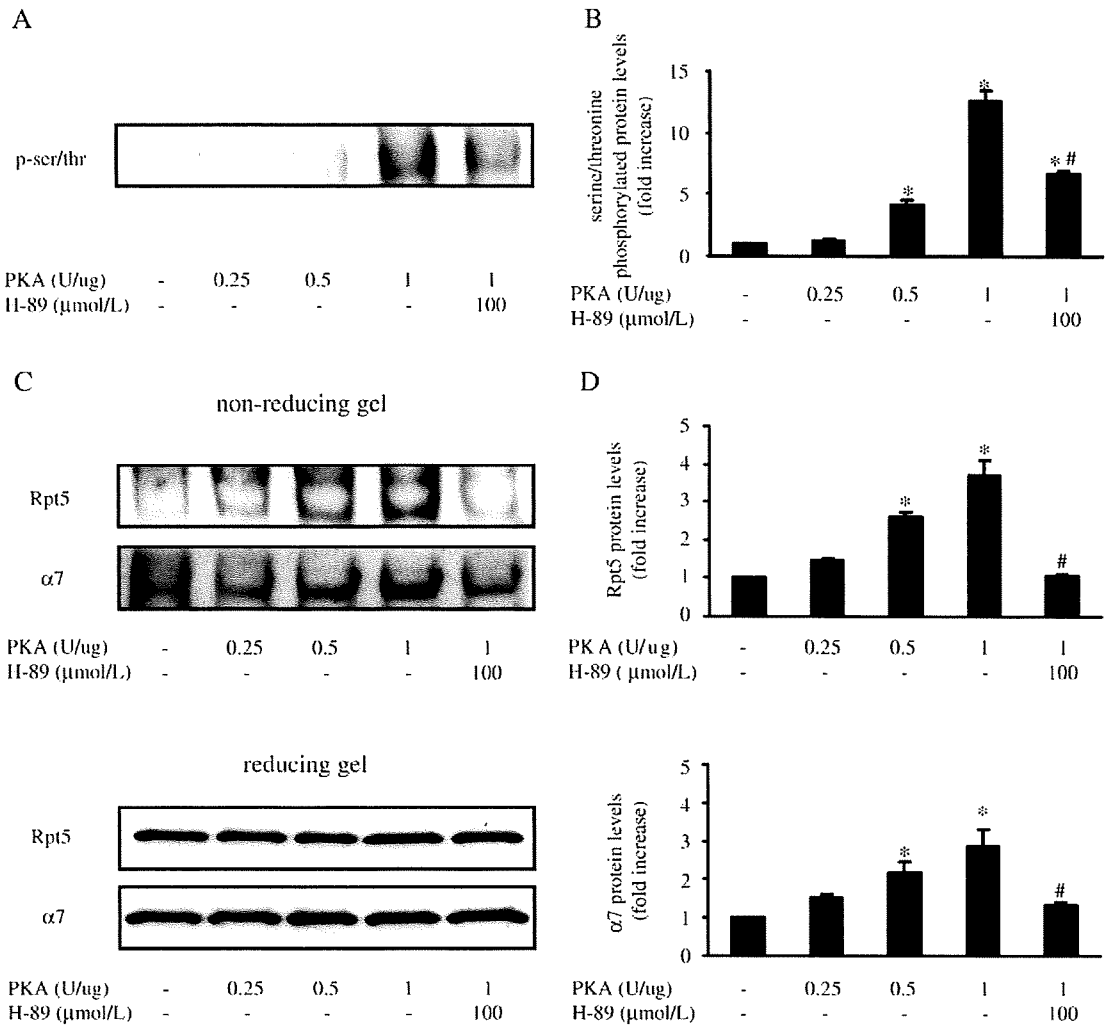

Fig. 2. PKA enhanced the activity of purified 26S proteasome. (A) Purified 26S proteasome activity detected by the in vitro proteasome peptidase assay. (B) Representative example of the 26S proteasome activity detected by in-gel peptidase assay using non-reducing gel electrophoresis. Purified 26S proteasome (1 μg) was applied to each lane. (C) Quantitative analysis of the 26S proteasome activity detected by in-gel peptidase assay. *$p<0.05$ vs. control, #$p<0.05$ vs. PKA (1 U/μg). $n=5$ per each group. Values are normalized to controls.

were incubated in assay buffer (50 mmol/L Tris–HCl, pH 7.5, 20 mmol/L $MgCl_2$, 1 mmol/L DTT, 50 μmol/L ATP) at 35 °C for 30 min. Then, they were incubated with proteasome activity assay buffer (50 mmol/L HEPES(pH 7.5), 5 mmol/L MgCl2, and 1 mmol/L DTT, 50 μmol/L ATP, 40 μmol/L LLVY-AMC) for 2 h at 37 °C. The fluorescence of each solution was measured by spectrophotometry (HitachF-2000; Hitachi Instruments, Tokyo, Japan) with excitation at 390 nm (Ex) and emission at 460 nm (Em). All readings were standardized relative to the fluorescence intensity of an equal volume of free 7-amino-4-methylcoumarin (Sigma) solution (40 μmol/L).

2.2.2. In-gel peptidase assay

The purified 26S proteasome with different treatments were separated by non-reducing native PAGE using a modification of the method described previously [13]. We used a four gel layer consisting of equal amounts, from the bottom up, of 7.5, 5, 4, and 3% polyacrylamide. Non-reducing gels were run at 125 V for 2.5 h. The gels were incubated on a rocker for 1 h at 37 °C with 15 mL of 0.4 mmol/L Suc-LLVY-AMC in buffer (50 mmol/L Tris–HCl, pH 7.5, 5 mmol/L $MgCl_2$, 50 μmol/L ATP). Proteasome bands, whose density indicates 26S proteasome activity, were visualized on exposure to UV light and were photographed.

2.3. Evaluation of proteasome phosphorylation and assembly in vitro

MThe purified 26S proteasome with different treatments were separated by non-reducing native PAGE described above. Proteins on the non-reducing gels were transferred (110 mA) for 1.5 H onto polyvinylidene difluoride membranes. Western blotting analysis was carried out sequentially for detection of changes in phosphorylation state with anti phospho-serine/threonine antibody and for detection of 26S proteasome with anti Rpt5 or α7-subunit antibody. Antigens were visualized by a chemiluminescent horse-radish peroxidase method with the ECL reagent. A parallel reducing gel was used to confirm the total amount of 26S proteasome.

2.4. Animal instrumentation

Beagle dogs (Oriental Yeast, Osaka, Japan) weighing 8 to 12 kg were anesthetized with sodium pentobarbital (30 mg/kg, intravenously), and were prepared as previously described [14]. Briefly,

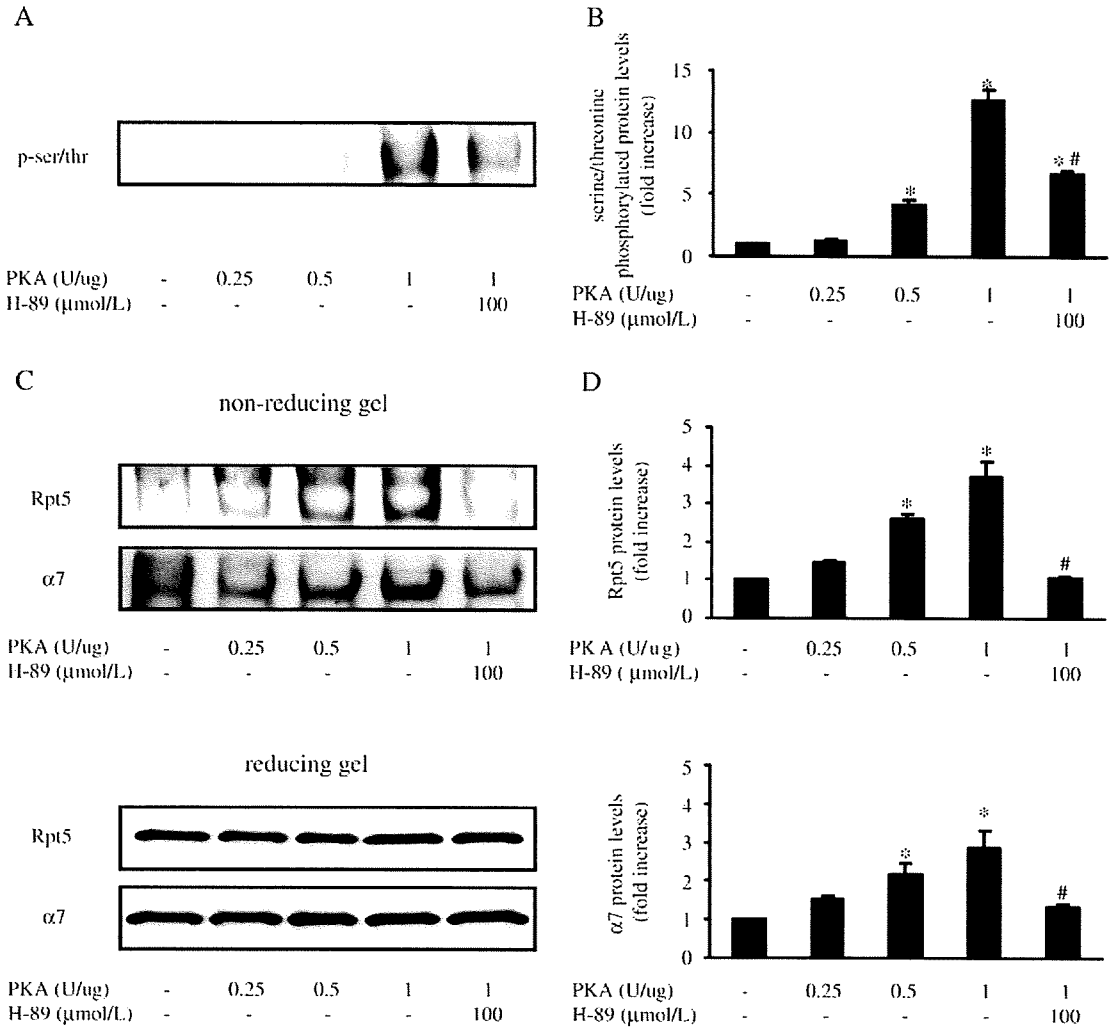

Fig. 3. PKA enhanced the phosphorylation and assembly of purified 26S proteasome. Representative example (A) and quantitative analysis (B) of 26S proteasome phosphorylation by Western blotting analysis with an anti phospho-ser/thr antibody. Representative example (C) and quantitative analysis (D) of Western blotting analysis on non-reducing gels. The status of 26S proteasome assembly was evaluated by Western blotting analysis with an anti-Rpt5 or anti-α7 antibody. Equal amounts of samples were loaded onto reducing and non-reducing gels. *$p<0.05$ vs. control, #$p<0.05$ vs. PKA (1 U/μg). $n=5$ per each group. Values are normalized to controls.

the trachea was intubated and each dog was ventilated by using room air mixed with oxygen. The chest was opened through the left fifth intercostal space, and the heart was suspended in a pericardial cradle. After heparinization (500 U/kg), the proximal portion of the left anterior descending coronary artery (LAD) was cannulated and perfused with blood via the carotid artery through an extracorporeal bypass tube. Both the coronary perfusion pressure (CPP) and heart rate (HR) were monitored during the experiments. In all experiments, CPP and HR were set at about 100 mmHg and 130 beats per min, respectively. This model was used to allow selective administration of agents to the LAD and reproduction of ischemia/reperfusion by clamping the bypass tube [15–17]. To examine the effects of PKA on proteasome activity in vivo, we employed isoproterenol or forskolin for exogenous stimulation of PKA and ischemic preconditioning (IP) for endogenous stimulation because PKA was reported to be activated by IP in canine hearts [15]. All procedures were performed in conformity with the Guide for the Care and Use of Laboratory Animals (NIH Publication No. 85-23, 1996 revision) and were approved by the Osaka University Committee for Laboratory Animal use.

2.5. Animal study protocols

2.5.1. Protocol I: Effects of isoproterenol or forskolin on proteasome activities in canine hearts

To assess the effects of exogenous PKA stimulation on proteasome activity, we selectively administrated saline ($n=4$), isoproterenol ($n=5$) or forskolin ($n=5$) into the LAD for 30 min in dogs. We preliminarily confirmed that the dose of ISO (10 μmol/L) used increased cAMP levels in the myocardium perfused by the LAD, but not in the myocardium of the left circumflex coronary artery (LCx) (data not shown). We determined the dose of forskolin (0.3 μg/kg/min) that activates PKA in canine hearts according to the previous report [18]. After administration, we rapidly sampled myocardial tissue from the LAD- and LCx-perfused myocardium as saline- or drug-treated myocardium and control one, respectively. Samples were placed into liquid nitrogen and stored at −80 °C (Fig. 1).

2.5.2. Protocol II: Effects of IP on proteasome activity in canine hearts

To assess the effect of endogenous PKA stimulation on the proteasome activity, we performed 4 cycles of 5 min coronary artery occlusion and a subsequent 5-minute period of reperfusion (IP) with

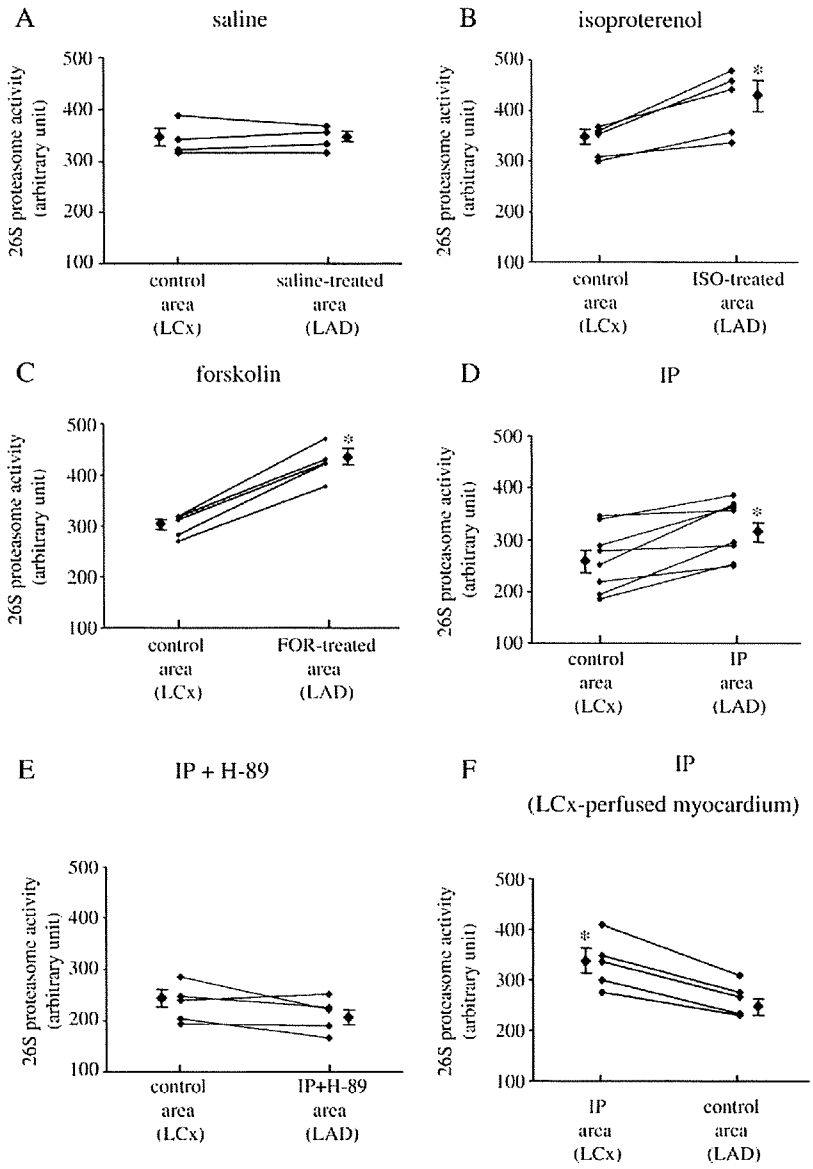

Fig. 4. Exogenous and endogenous PKA stimulation increased 26S proteasome activity in canine hearts. (A) 26S proteasome activity of canine hearts after sham operation in the control (LCx) or saline-treated (LAD) myocardium (n=4). (B, C) Effects of the exogenous PKA stimulation by the intracoronary administration of isoproterenol (ISO) or forskolin (FOR) on 26S proteasome activity in canine hearts (n=5). Effects of the endogenous PKA stimulation by ischemic preconditioning (IP) with saline (D) or H-89 (E) on 26S proteasome activity in canine hearts (n=8 and 5, respectively). (F) Effects of IP on 26S proteasome activity in the LCx-perfused myocardium (n=5) *p<0.05 vs. control area.

the intracoronary administration of saline (n=8) or H-89 (1.35 μg/kg per min) (n=5) for 50 min in dogs. The dose of H-89 was selected because the previous study showed this dose of H-89 inhibited the PKA activity in canine hearts [15,16]. At 30 min after IP, we rapidly sampled tissues from the LAD- and LCx-perfused myocardium, placed the samples into liquid nitrogen, and stored them at −80 °C. To confirm that proteasome activation by IP was not dependent on the myocardial area, we also performed the same IP protocol in LCx-perfused myocardium instead of LAD-perfused one in 5 dogs (Fig. 1).

2.5.3. Protocol III: Time-course changes in proteasome activity during ischemia/reperfusion period in canine hearts

To assess the time-course changes in proteasome activity during ischemia/reperfusion period in canine hearts, we underwent 90 min of ischemia followed by 6 h of reperfusion with and without IP in 10 dogs. Myocardial biopsy specimens were taken from LAD-perfused myocardium in each canine at 4 time-points: at the control, just before ischemia (pre-ischemia), at the end of 90 min ischemia (post-ischemia) and 6 h of reperfusion (post-reperfusion) (Fig. 1).

Fig. 5. PKA stimulation did not alter total protein levels of proteasome subunit in canine hearts. Representative example and quantitative analysis of Western blotting analysis of protein levels for 19S proteasome subunit Rpt5 as well as 20S proteasome subunits α7 and β5 in canine hearts after saline treatment (A), isoproterenol (ISO) treatment (B), forskolin (FOR) treatment (C), ischemic preconditioning (IP) (D), IP with H-89 (IP+H-89) (E). IP was performed in the LCx-perfused myocardium (F) instead of LAD-perfused one. CON and MW indicate control and molecular weight, respectively.